CONDUCTION MECHANISMS IN THICK FILM MICROCIRCUITS

R. W. Vest

Purdue Research Foundation

Prepared for:

Advanced Research Projects Agency

31 December 1974

Semi-Annual Technical Report
for the Period 7/1/74-12/31/74

CONDUCTION MECHANISMS IN THICK FILM MICROCIRCUITS

Grant Number: DAHC15-73-G8

ARPA Order No.: 1001/192

Grantee: Purdue Research Foundation

Principal Investigator: R. W. Vest
(317) 749-2601

Effective Date of Grant: 7/1/73

Grant Expiration Date: 6/30/75

Amount of Grant: $ 77,923

February 1, 1975

Forward

Research described in this report constitutes the ninth six months effort under two grants from the Defense Advance Research Projects Agency, Department of Defense, under the technical cognizance of Dr. Norman Tallan, Aerospace Research Laboratories, U. S. Air Force. Copies of previous reports are available from Defense Documentation Center, Cameron Station, Alexandria, VA., 22314. The research was conducted in the Turner Laboratory for Electroceramics, School of Electrical Engineering and School of Materials Engineering, Purdue University, West Lafayette, Indiana 47907, under the direction of Professor R. W. Vest. Contributing to the project were Assistant Professor G. L. Fuller, Messrs. D. J. Deputy, A. N. Prabhu, and R. L. Reed. The level of effort was drastically reduced, beginning January 1, 1974, so that sufficient funds would be available for two graduate students to complete their thesis research under the one year, no cost, time extension granted by ARPA.

Abstract

The sintering kinetics and the ripening kinetics for RuO_2 particles in the presence of a glass phase were studied by measuring surface area, X-ray line broadening, shrinkage, and electrical resistance. Results from these four (4) techniques are interpreted in terms of competing processes which occur during thick film resistor firing. The sheet resistance of thick film resistors as a function of RuO_2/glass ratios is reported.

TABLE OF CONTENTS

LIST OF FIGURES

I. Introduction

Advances in thick film technology have been hindered by an inadequate understanding of the relationships between the physical properties of the ingredient materials and the electrical properties of the resulting resistors and conductors. The lack of a predictive model of the conduction mechanism has hampered the development of new materials, as well as the improvement of existing systems. The two primary concerns of the present research program in the area of resistor technology are the development of adequate models to describe the "Blending Curve Anomaly" and the "TCR Anomaly." The "Blending Curve Anomaly" refers to the often reported observation that with oxidic conductors and glass the sheet resistance varies monotonically from very low (e.g., 2 v/o) to very high conductive concentrations; whereas, with noble metal conductives and glass electrical continuity is not achieved until the amount of conductive approaches 30 v/o or higher. The primary scientific question is: what are the driving forces which are responsible for the formation of continuous conducting paths along the length of the resistor at such low concentrations of the conductive? The "TCR Anomaly" refers to the fact the temperature coefficient of resistance of a resistor is much lower than the TCR of any of the individual ingredients from which it was made. The primary scientific question is: what is the mechanism by which electric charge is transported?

The primary thrust of the experimental program is to relate electrical properties of the thick films to the materials properties and processing conditions through microstructure. The materials properties to be correlated

are: resistivity, temperature coefficient of resistivity, coefficient of thermal expansion, interfacial energy, particle shape, size and size distribution, and chemical reactivity with other constituents. The processing conditions to be correlated are time, temperature and atmosphere during firing. The specific objectives of the program are:

1. Determine the dominant sintering mechanisms responsible for microstructure development and establish the relative importance of the various properties of the ingredient materials.
2. Dete ine the dominant mechanisms limiting electrical charge transport, and establish the relative importance of the various properties of the ingredient materials.
3. Develop phenomenological models to interrelate the various materials properties with systems performance.

Earlier work in these three areas have been previously reported [1-8].

II. Microstructure Development

The electrical properties of a thick film resistor depend directly on the microstructure that is formed during the firing cycle, normally executed as a continuous process in a tunnel kiln. The proposed model of microstructural development [9] predicts a sequence of steps involving sintering of the glass; wetting the conductive particles, attraction of the conductive particles to form a continuous network, sintering of the conductive particles, and, finally, destruction of the conductive network. Studies described in this report were directed toward elucidating the last two steps.

A. Surface Area and X-Ray Line Broadening.

In the previous report [10], the reasons for employing secondary techniques rather than direct observation of neck growth and density measurements to obtain information on the liquid phase sintering and/or ripening of RuO_2 particles in the presence of the molten glass were discussed. The secondary techniques discussed were microstructure evaluation, X-ray diffraction line broadening and surface area measurements. Further experiments were carried out, utilizing the above techniques to obtain additional data.

Samples were prepared by heating a mixture of RuO_2 and glass (63% PbO-25% B_2O_3-12% SiO_2) powders (30 wt.% RuO_2) for varying times in a platinum crucible after they were thoroughly dispersed in the agate mill. The RuO_2 powder used has been previously characterized [11]. The firing temperatures employed were 800, 850, 900, 950 and 1000°C. After firing, all

of the glass was completely leached out and only the RuO_2 remaining was used for the analysis.

The surface area measurements were carried out using an Aminco Sor BET helium carrier surface area meter. The average crystallite sizes were determined by X-ray diffraction line broadening techniques on powder samples, using a Siemens diffractometer; 3 different peaks (110, 101 and 211) were scanned, using copper radiation at a speed of 1/100 degree/minute to investigate the possibility of different growth behavior in different directions.

For analysis of the X-ray data integral line breadth was used in the Scherrer equation instead of the half maximum line breadth. Corection for instrumental and Kα-doublet broadening were carried out according to the method outlined by Kaeble [12]. The pure diffraction breadth was obtained by the graphical method from the curve corresponding to skewed distribution of crystallite sizes [13].

The average crystallite sizes obtained from X-ray data were also taken as average particle sizes for the reasons explained in the previous report [14]. The surface area data were converted to average particle size assuming all the particles to be uniform size spheres. The results obtained with both techniques are plotted in Figs. 1-5 for the five temperatures.

The minor differences in the average particle sizes obtained from the X-ray data shown in Figs. 1-5 as compared to those presented in the previous report [15] are due to the differences in the method of calculation. The growth pattern in all the three directions studied seems to be similar. The main feature to be noted is the shape of the curves and differences between the X-ray and surface area results, particularly with for long times

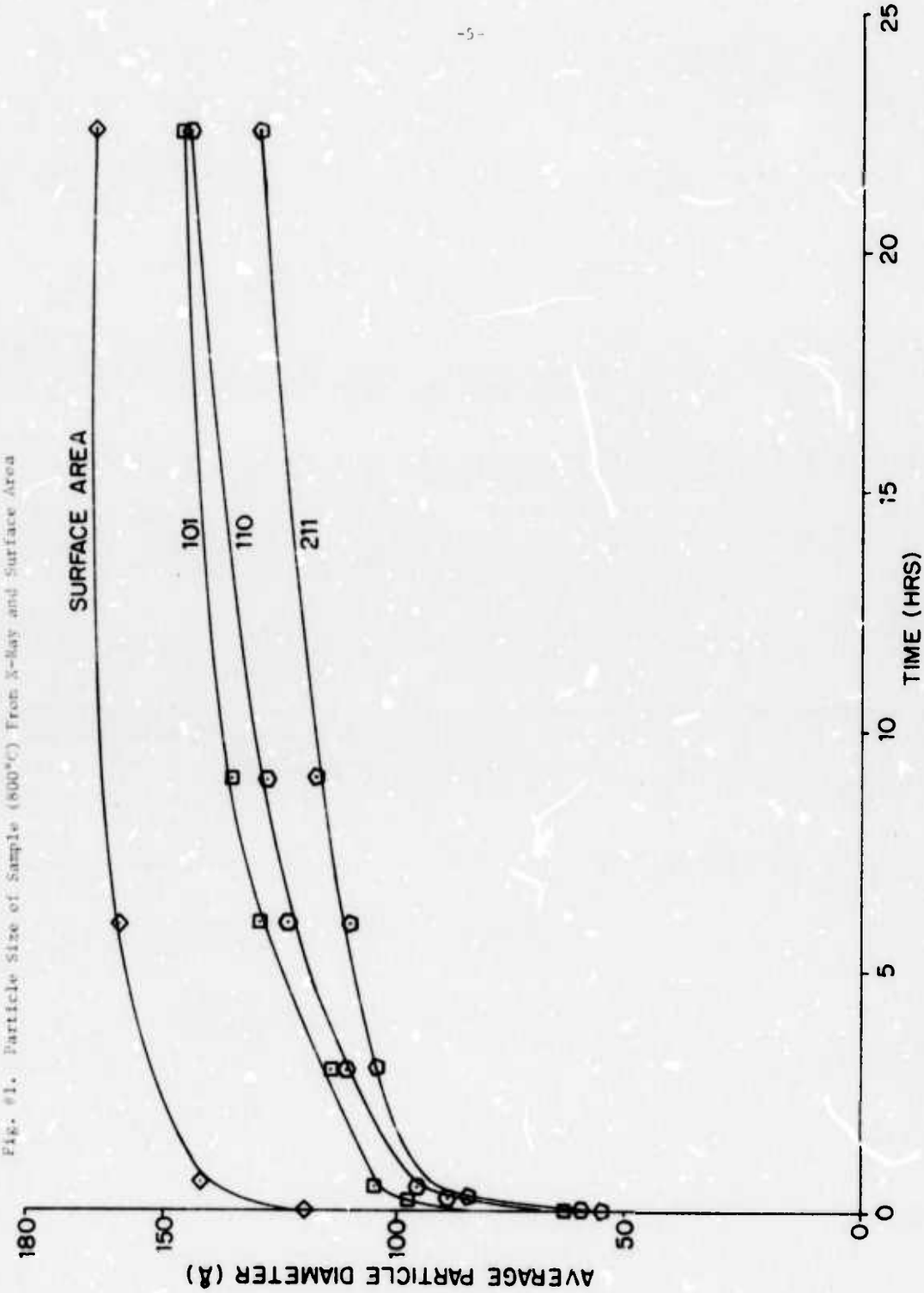

Fig. #1. Particle Size of Sample (800°C) From X-Ray and Surface Area

Fig. 62. Particle Size of Sample (850°C) From X-Ray and Surface Area

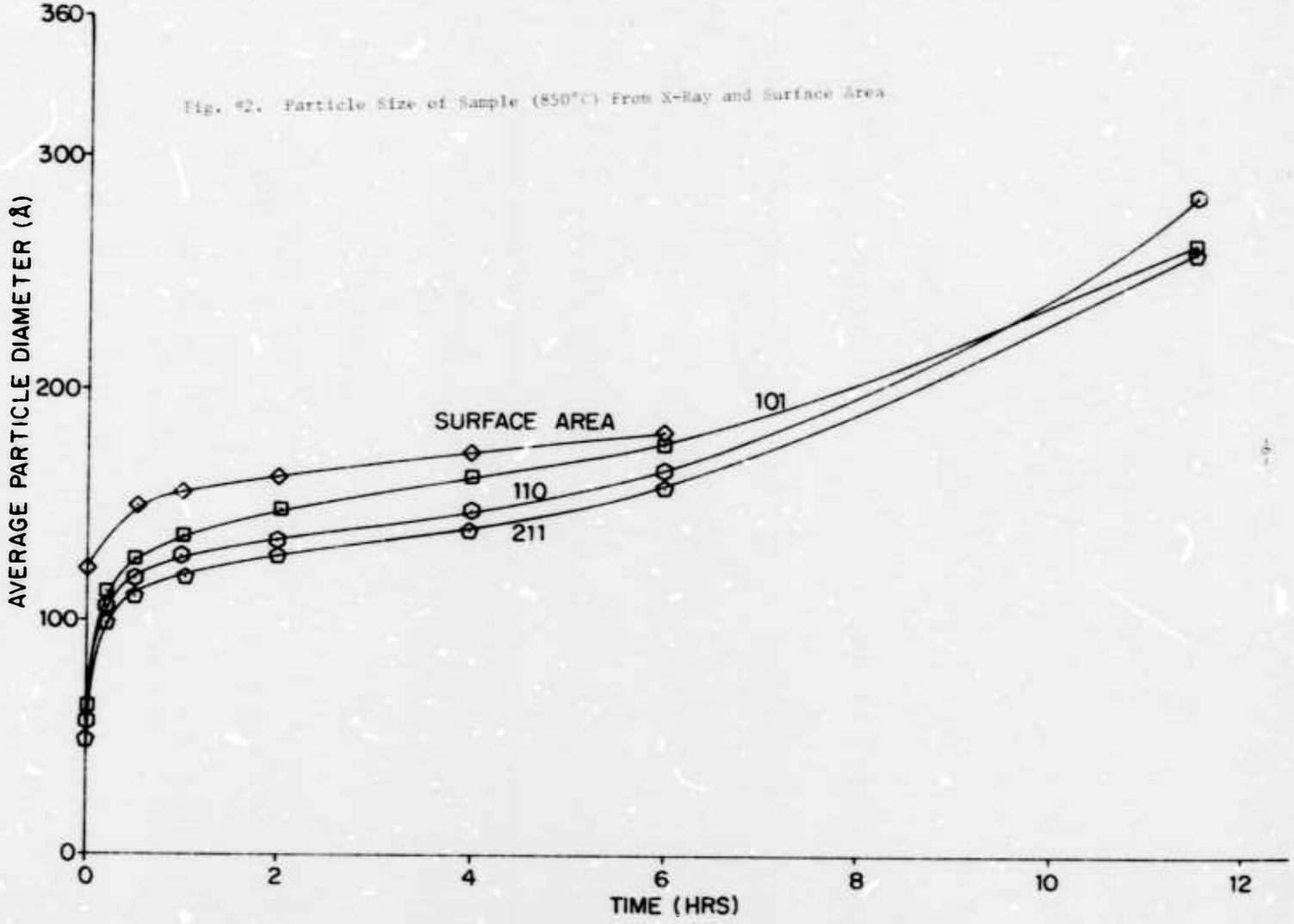

Fig. #3. Particle Size of Sample (900°C) From X-Ray and Surface Area

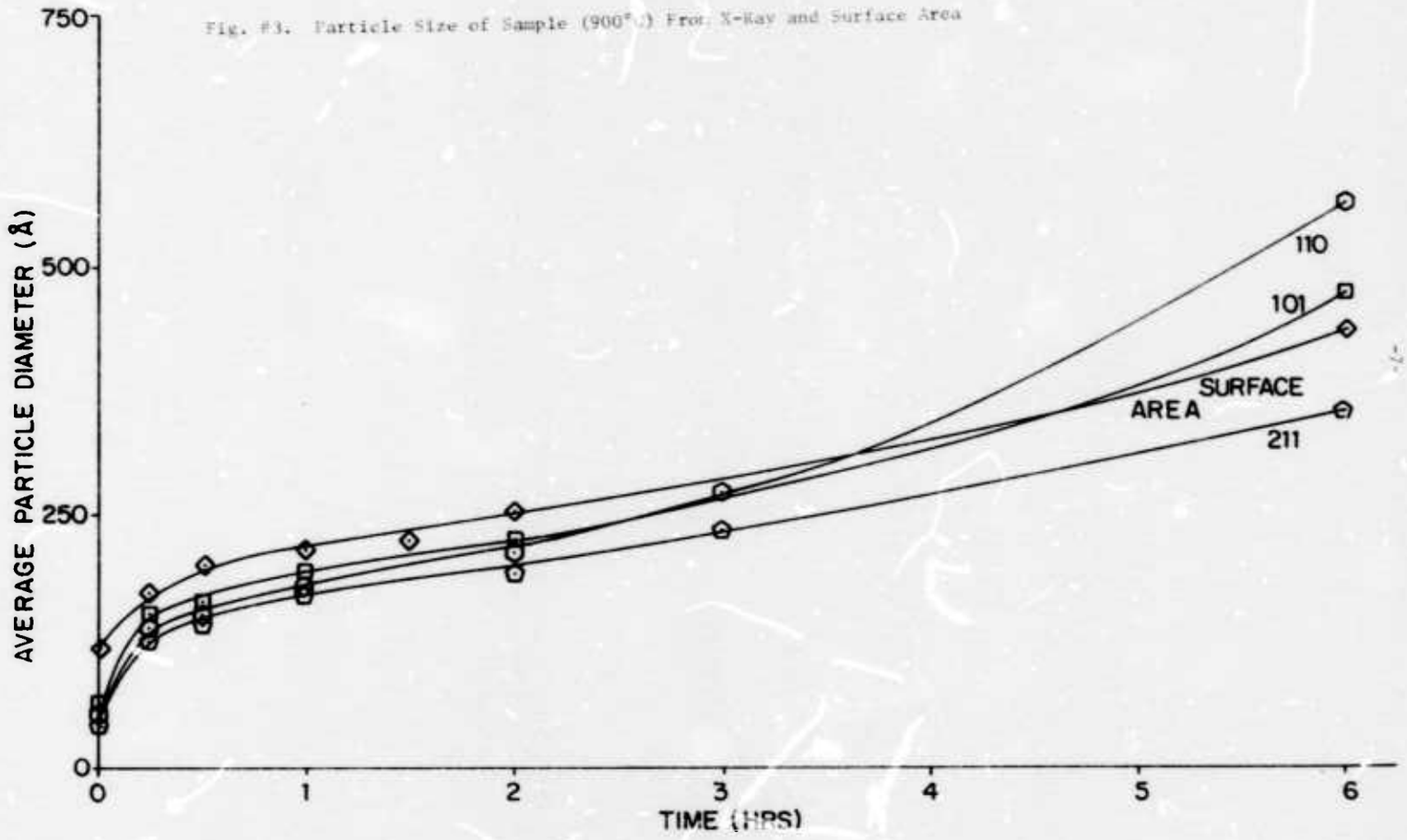

Fig. #4. Particle Size of Sample (950°C) From X-Ray and Surface Area

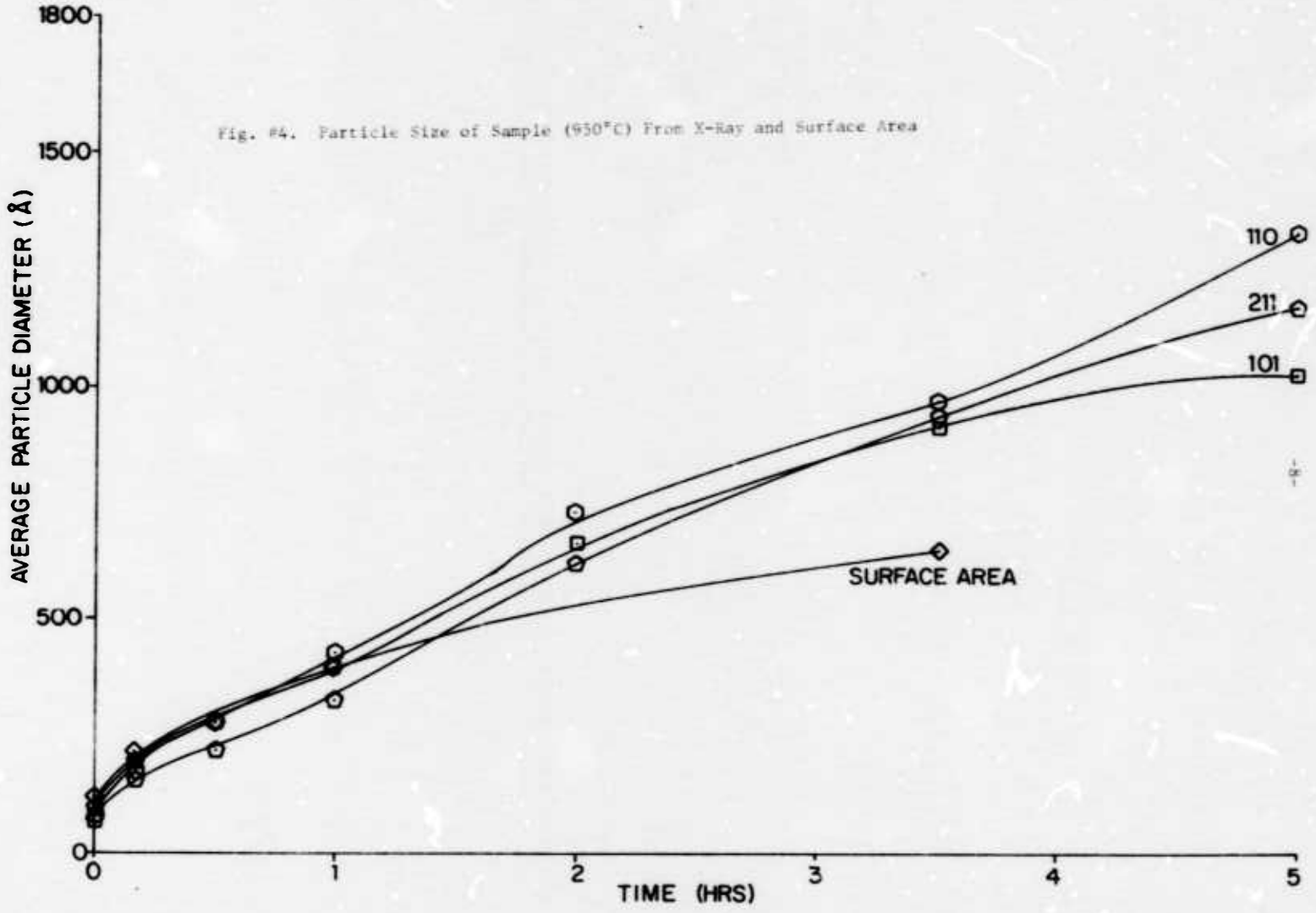

Fig. #5. Particle Size of Sample (1000°C) From X-Ray and Surface Area

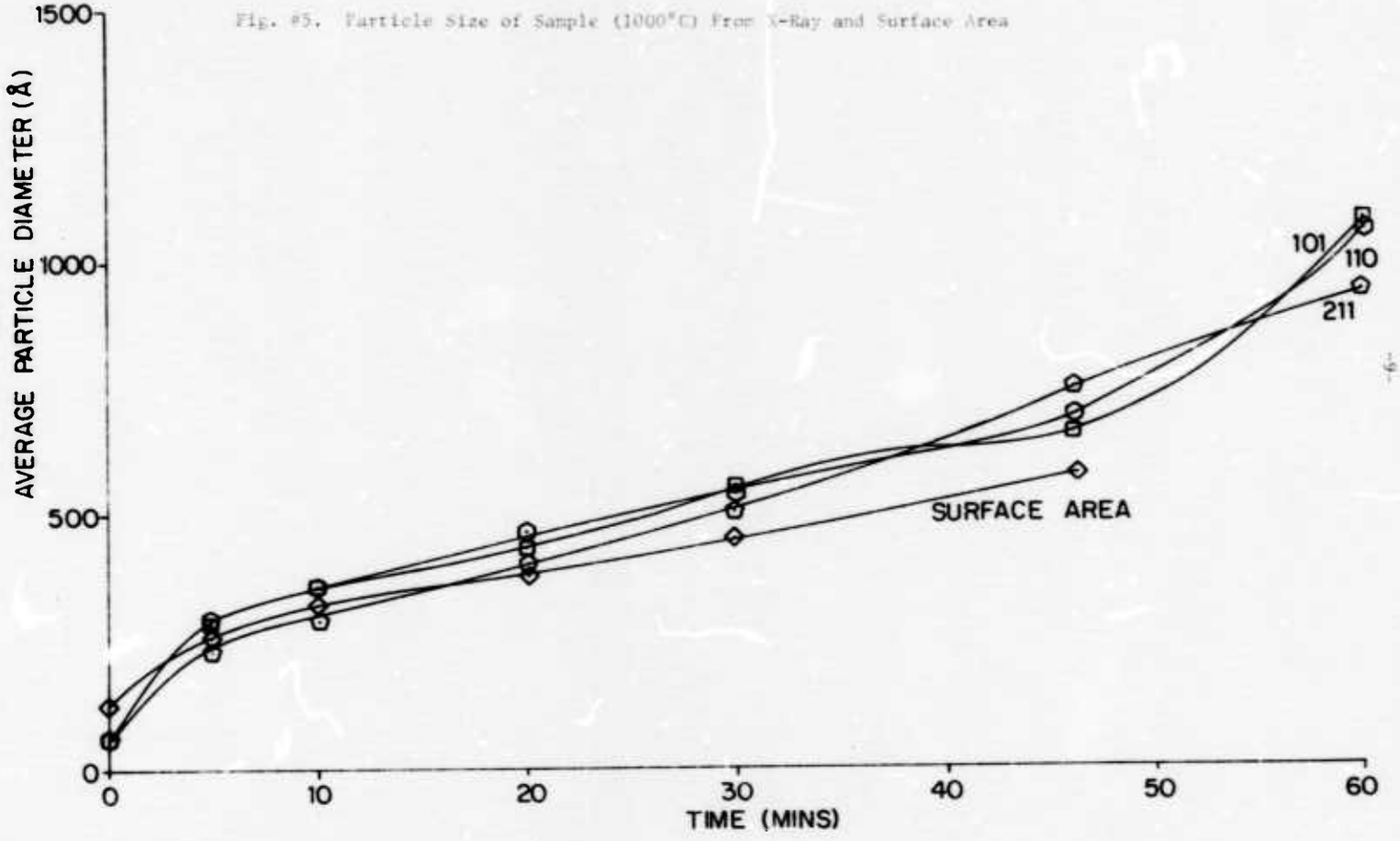

at 850, 900, 950 and 1000°C. There appears to be indications of exaggerated growth, as evidenced by the increased slopes of the curves derived from X-ray data, but this may be a result of the measuring technique. For a powder sample composed of crystallites of a wide distribution of sizes the size calculated from the line breadth is weighted towards larger sizes [16]. For cubic crystals, if there are n particles of size t,

$$\text{Observed mean size} = \frac{\Sigma nt^4}{\Sigma nt^3}$$

whereas, $$\text{true mean size} = \frac{\Sigma nt}{\Sigma n}$$

The difference between the observed and true mean sizes increases as the distribution becomes more wide, and particularly, if a few large crystallites and a large number of small crystallites are present. From previous electron microscope studies [17] of RuO_2-glass samples it is known that large crystallites of RuO_2 do grow under certain circumstances and this fact has to be taken into consideration while analyzing the data.

B. Electrical Resistance.

Results of experiments monitoring the resistance of resistors during firing have been described in previous reports [18]. Further experiments were carried out on resistance changes under isothermal conditions in order to obtain additional data that could give quantitative information on the different stages of network development of the thick film resistors. The samples were prepared by screen printing 40 w/o RuO_2 paste on the AlsiMag 614 (96% Al_2O_3) substrates. The samples were dired at 250°C for half an hour before the final heat treatment. Electrical resistance (DC) was measured,

using a four probe technique.

Two different types of measurements were carried out.

(1) The push rod furnace [19] was used to record the resistance changes under isothermal conditions. Since the different zones of the furnace are maintained at different temperatures, the maximum temperature the sample attains depends upon the extent to which it is pushed inside the furnace, and 5-10 minutes are required for the sample to reach thermal equilibrium.

The resistance changes as a function of time at different temperatures are shown in Fig. 6. The rapid initial decrease in resistivity is probably due to a rearrangement of the RuO_2 particles during the glass sintering, and to a formation of the intial particle-to-particle contacts. The initial decrease in resistivity is followed by a rapid increase. Such a feature has been observed in the Ag-PdO thick film resistor system [20], and was attributed to the oxidation of Pd to PdO. From earlier studies [21] utilizing the hot stage microscope with RuO_2-glass resistors it is known that there are a considerable number of gas bubbles formed at temperatures above the softening point of the glass. While the source of these gas bubbles has not been identified, the phenomenon has been observed in all cases, and a certain degree of disruption of the RuO_2 particles results from the motion of the gas bubbles. This disruption of the RuO_2 particles prior to the time when a sintered network is formed would result in an increase in resistance. The rapid increase in resistance is followed by a slow decrease in resistance, which can be associated with the sintering of RuO_2 at the higher temperatures. An increase in resistance can be observed at the longer times at 800°C. This increase can be associated with the ripening process.

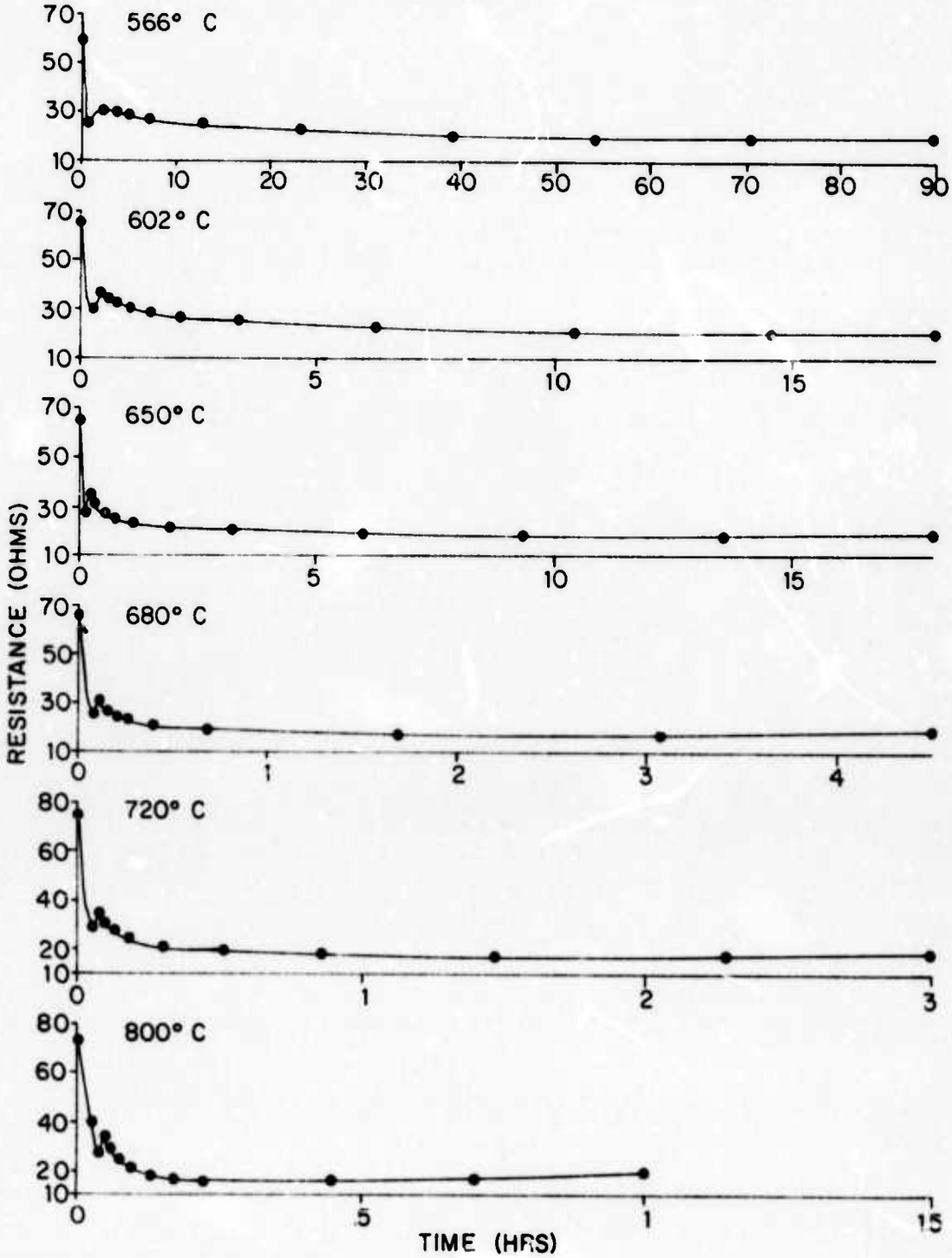

Fig. #6. Resistance Versus Time During Firing At Different Temperatures

(2) The second set of measurements involved changes in the room temperature electrical resistance of the samples after they were heated at 600, 625, 650, 675, 700, 800, 900 and 1000°C for varying times. The results, shown in Figs. 7 and 8, are similar to the high temperature results. Figure 9 gives a comparison of room temperature and high temperature resistance values as a function of time at three different temperatures.

The initial peak is seen only at 600° in the room temperature data; at the higher temperatures the peak occurs over such a short period of time that either the resistance has increased and decreased before the initial datum point is obtained, or the first datum point is before the peak and the second after the peak. At the higher temperatures (800, 900, and 1000°C) the initial stages occur in a very short time and the resistance increase (probably due to the ripening process) can be easily observed. At still longer times at the three highest temperatures the resistance is seen to decrease again. The reason for this decrease is not known, but two possibilities are: diffusion of the conductive (platinum) into the resistor region, or loss of the glass due to vaporization.

C. Shrinkage.

In the previous report [22], it was indicated that no appreciable dimensional changes occurred in the RuO_2-glass compacts, even after long hours of heating at 1000°C. This observation was attributed to closed pores inside the compacts. Since the dimensional measurements after cooling to room temperature did not yield the desired information about changes occurring during firing, it was decided to make shrinkage measurements under isothermal conditions, using the horizontal dilatometer [23].

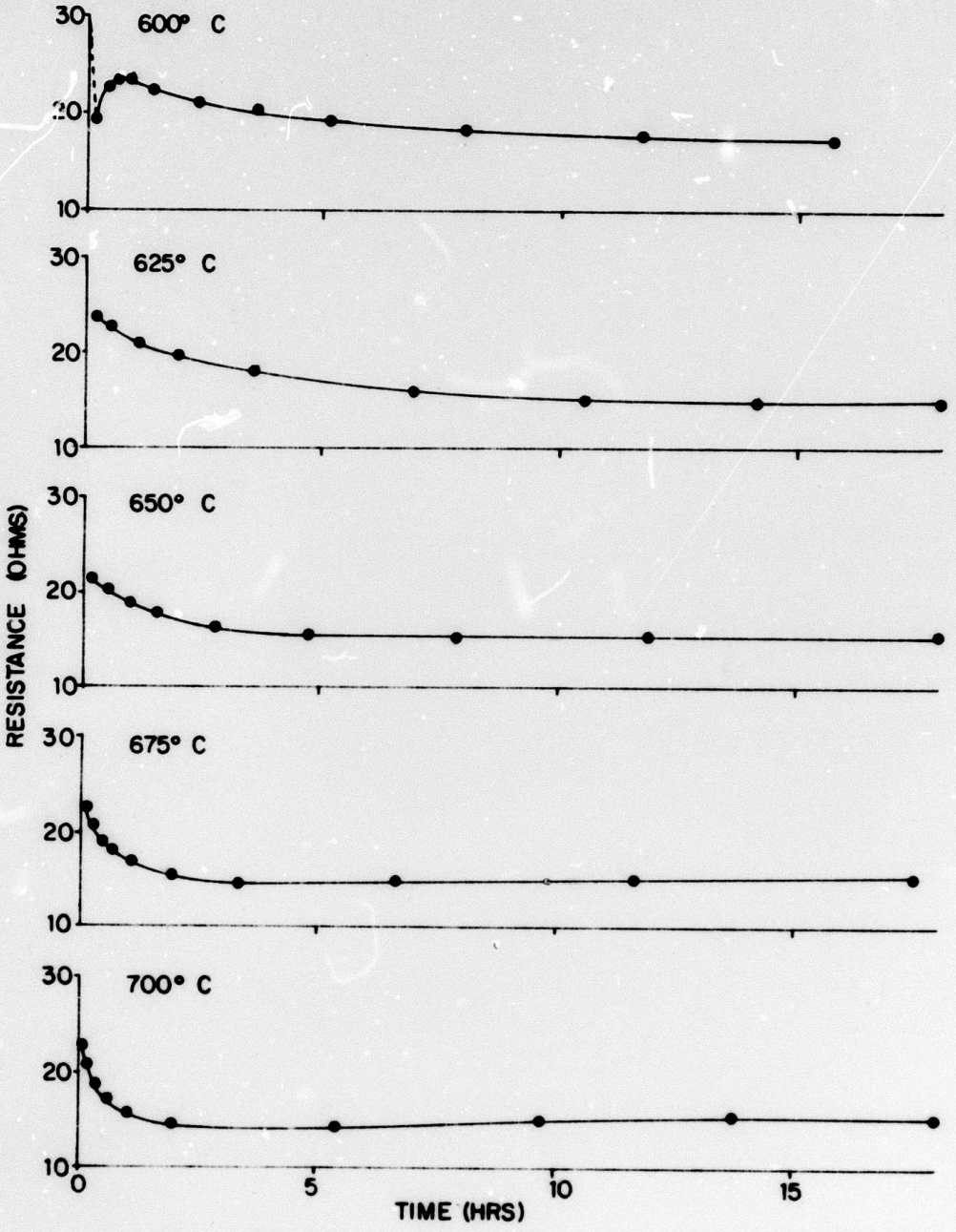

Fig. #7. Room Temperature Resistance Versus Time of Firing At Different Temperatures

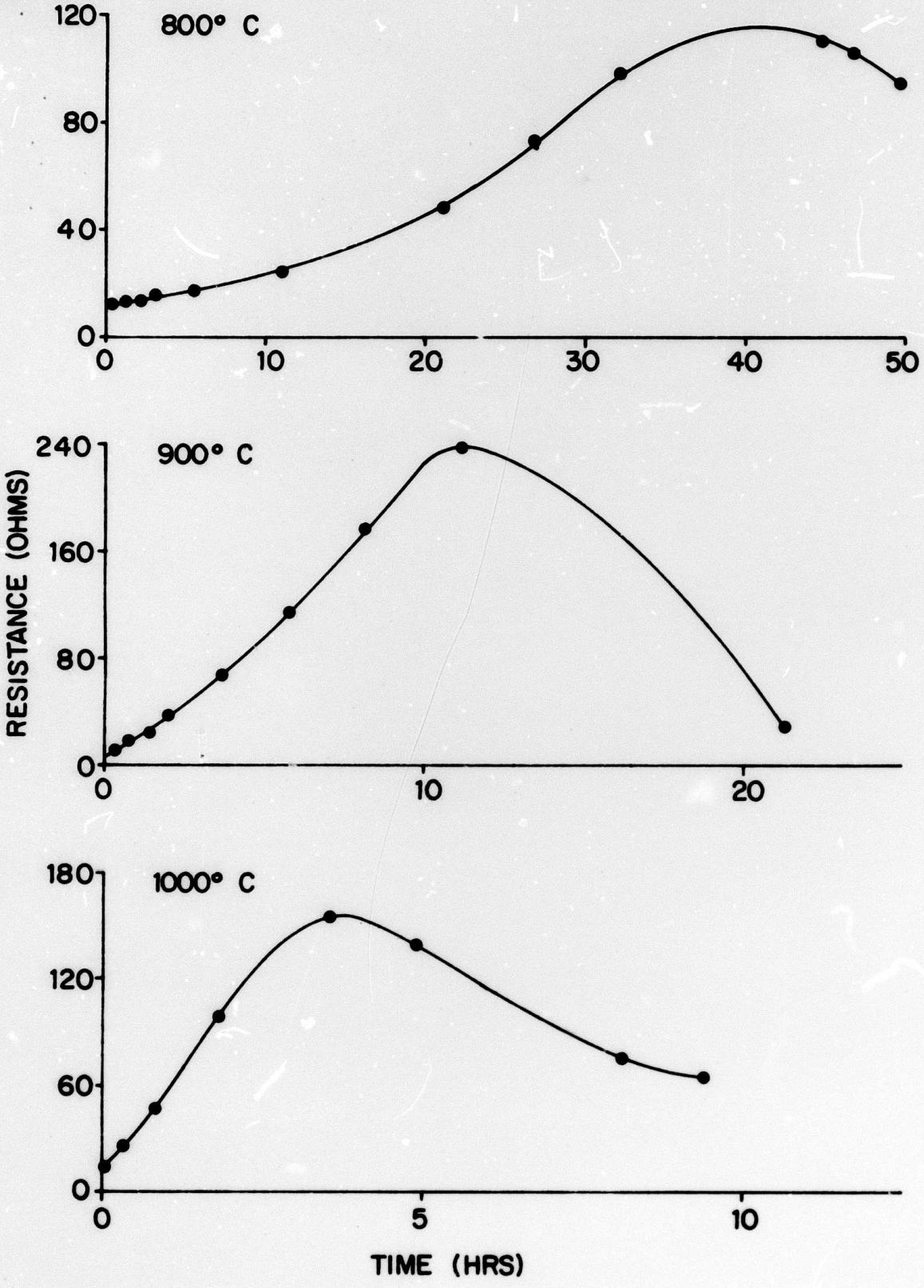

Fig. #8. Room Temperature Resistance Versus Time of Firing At Different Temperatures

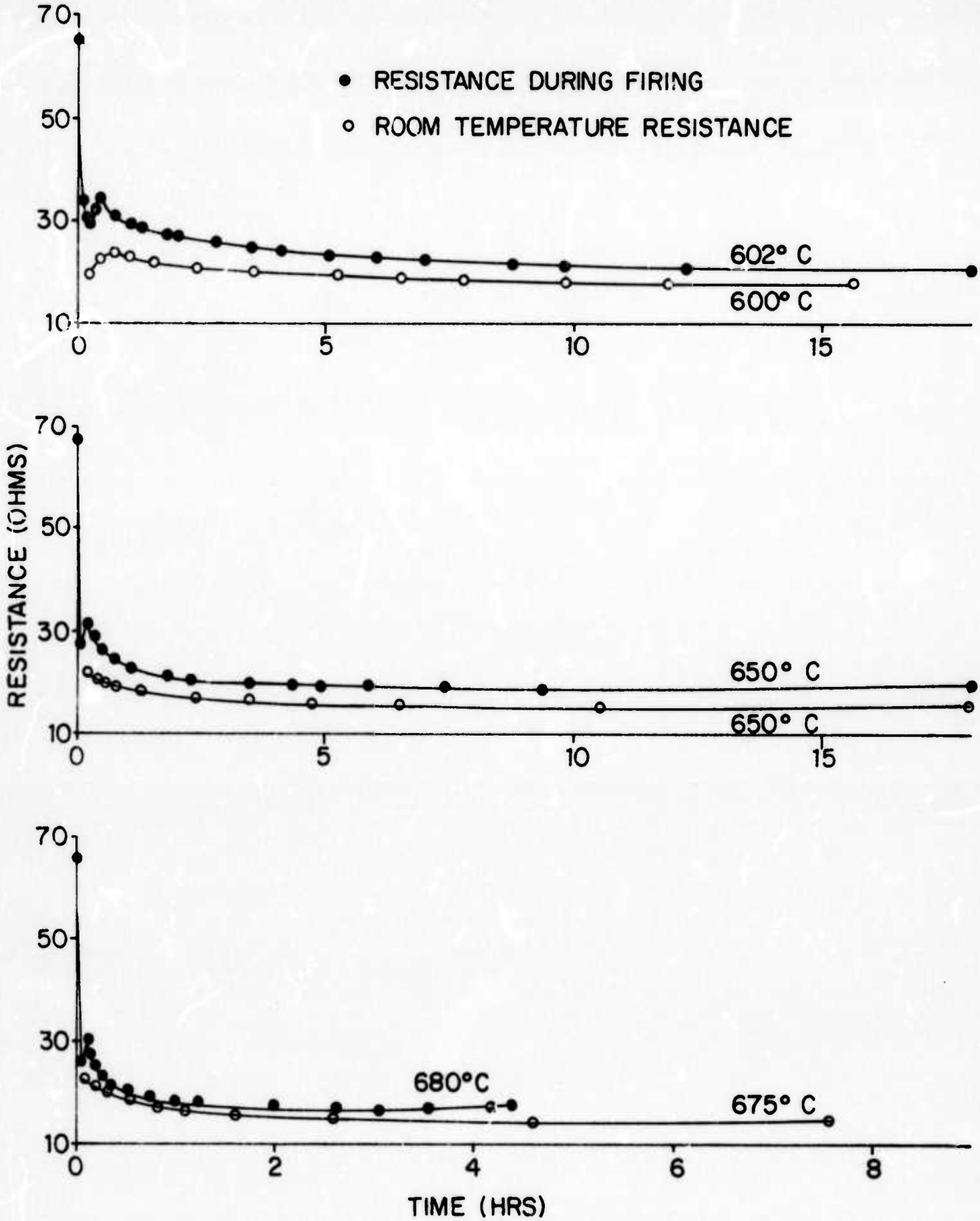

Fig. #9. Comparison Between Resistance Change During Firing and Room Temperature Resistance After Firing

Length changes occurring were recorded on a strip chart recorder with a sensitivity such that the full scale deflection of 10 inches on the recorder corresponded to 0.0005 inches of length change. With this sensitivity length changes as small as 5×10^{-6} inches could be easily detected.

The samples for shrinkage measurements were prepared in the following way: The mixture of RuO_2 and glass (30 w/o glass) was dispersed thoroughly and pressed in an uniaxial press at 60,000 psi. The as pressed samples were about 0.2 inches long and 0.25 inches in diameter. All the samples were preheated at 450°C for 1 hour. The purpose of this preheat treatment was to allow the initial rapid contraction due to loss of moisture, rearrangement, and glass sintering.

The shrinkage data for six different temperatures are shown as a function of time in Figure 10. Four stages can be identified in the time dependence of the relative shrinkage.

Stage 1 is an initial very rapid expansion shown at all six temperatures. This stage is simply the result of the thermal expansion of the sample as it approaches thermal equilibrium in the furnace.

Stage 2 is a contraction which occurs: (1) over the full time span measured at 565 and 605°; (2) up to at least 6 or 7 hours at 648°; (3) up to 20, 5 and 2 minutes at 695, 722 and 752°C respectively. This contraction is most probably due to a rearrangement and initial stage sintering of the RuO_2 particles in the presence of the glass.

Stage 3 is an expansion which can be observed: (1) as a slight increase in relative length at the longest times at 648°C; (2) at 695°C over the time period 20 minutes to 2.5 hours; (3) at 722°C over the time

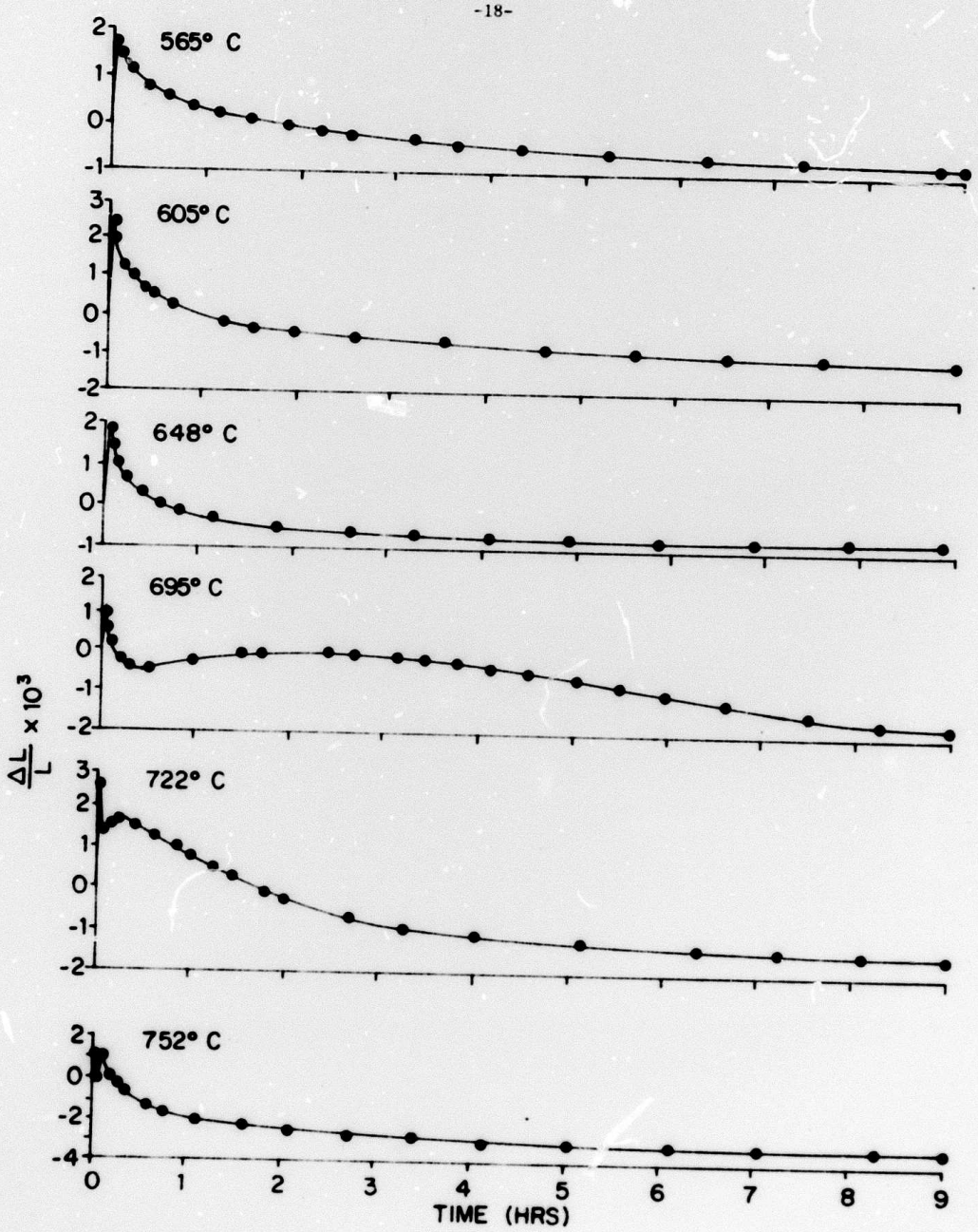

Fig. #10. Relative Shrinkage Versus Time of Heating At Different Temperatures

period 5 to 15 minutes; (4) at 752°C over the time period 2 minutes to 5 minutes. Data at the very short times do not have quantitative significance because approximately 10 minutes are required for the sample to reach thermal equilibrium. It is believed that stage 3 is associated with the formation and expension of gas bubbles in the glass. The phenomenon is not observed at the lower temperatures because the glass does not have closed pores, and is observed only at very short times at the higher temperatures because the glass viscosity has decreased to a sufficiently low value that the gas bubbles are released as rapidly as they are formed.

Stage 4 is a further contraction which is observed after 2.5 hours at 695°C, after 15 minutes at 722°C, and after 5 minutes at 752°C. It is believed that this stage is a continuation of the sintering of the RuO_2 in the presence of the glass. Weight change measurements have shown that the loss of RuO_2 and/or glass by vaporization is insufficient to account for the observed dimensional changes during stage 4.

III. Charge Transport

A. Blending Curve.

End member thick film resistor formulations were prepared by combining 5 wt.% (3.3 vol.%) RuO_2 to glass and 40 wt.% (30.2 vol.%) RuO_2 to glass powders with a 5% ethyl cellulose in butyl carbitol screening agent. The RuO_2 and glass (63% PbO-25% B_2O_3-12% SiO_2) powders used were those previously characterized [11]. Intermediate value resistor formulations (10, 20, 30 wt.%) were prepared by combining suitable aliquots of the two end members. Each formulation was blended on the 3-roll laboratory mill described previ-

ously [24]; this mill has recently been modified by fitting fused silica sleeves to the stainless steel rolls, thereby insuring that the only contamination to the formulation during the milling operation would be SiO_2. The rheology of the formulations was adjusted to the specifications previously developed [25]. Platinum conductives (Engelhard No. 6082) were printed on AlSiMag 614 (96% alumina) substrates 1/2" x 1/2" x 0.025", and fired. The resistors were then printed on these electroded substrates in a one-square pattern (0.175" x 0.175") using a modified Aremco semi-automatic screening machine [26] and a 165 mesh stainless steel screen. The settings for snapoff distance, squeegee overtravel, and squeegee speed were those which had been determined to be optimum during the earlier studies of repeatability of screen printing [27]. The screened resistors were dried in a laboratory type oven for 15 minutes at 130°C to remove the volatile organics and then fired in a Lindberg tunnel kiln, using the time-temperature profile previously shown [28] to give minimum scatter in resistance values. Resistance of each of the resistors was determined by a 4-terminal measurement technique, averages and standard deviations calculated, and the sheet resistance normalized to a resistor thickness of 0.001". These data are given in Table 1 and are plotted in Figure 11.

Table I. Blending Curve Data

	wt.% (vol.%) RuO_2/RuO_2 + glass				
	5 (3.3)	10 (6.7)	20 (14.0)	30 (21.7)	40 (30.2)
Number of Resistors	11	11	11	11	11
Average Sheet Resistance (KΩ/square)	157.15	2.986	0.1669	0.04087	0.01317
Standard Deviation (KΩ/square)	56.88	0.696	0.01242	0.00190	0.00038
Standard Deviation (%)	36.2	23.3	7.4	4.6	2.9
Normalized Sheet Resistance (KΩ/square-mil)	106.86	2.120	0.1605	0.0358	0.01304

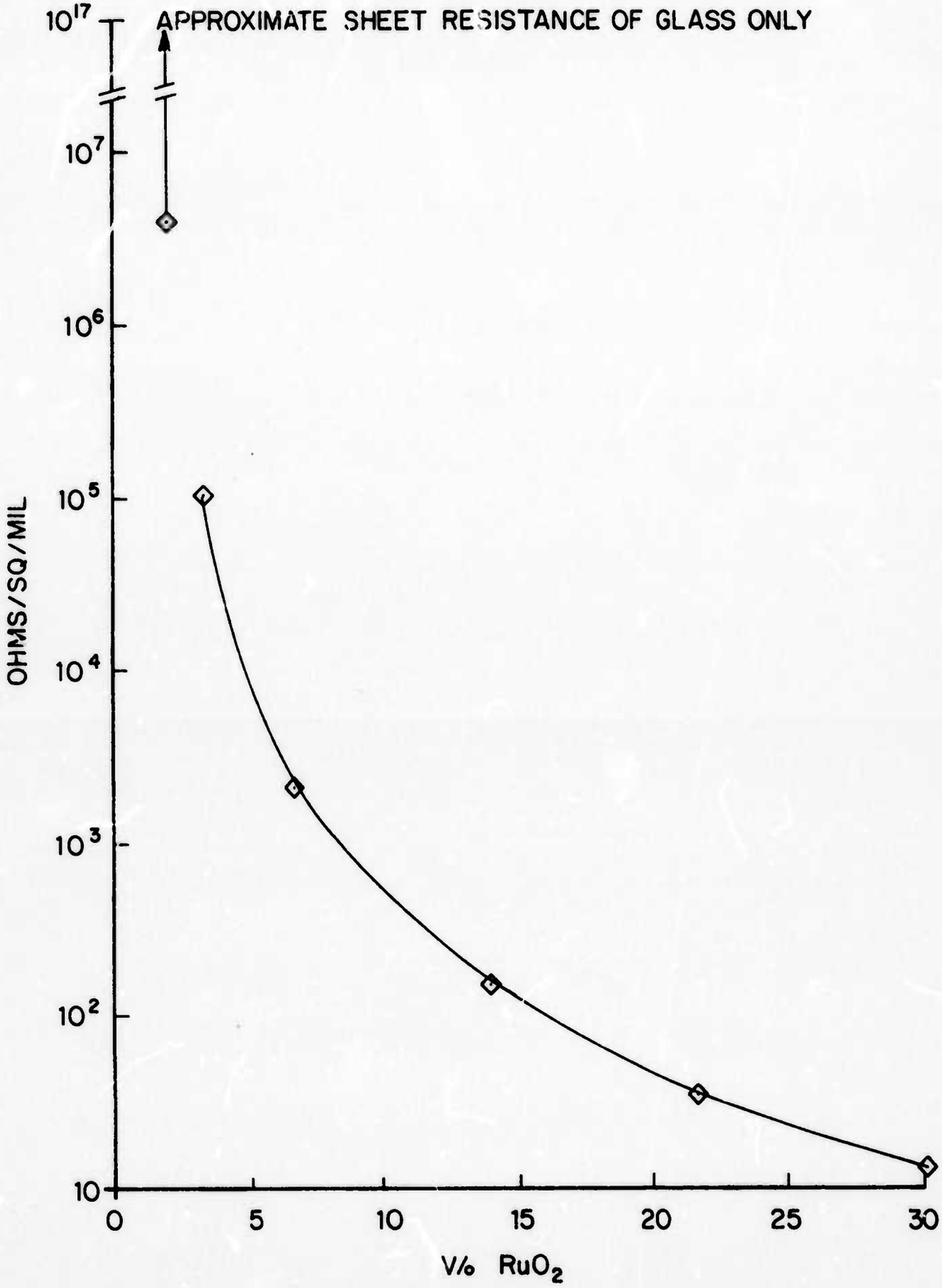

Fig. #11. Blending Curve for 30.2 V/o and 3.3 V/o RuO_2 End Members

Attempts were made to prepare higher value resistors by blending the 5 wt.% end member with a glass-screening agent combination to obtain 1.5 and 3 wt.% (1 and 2 vol.%) RuO_2 to glass. All resistors made from the 1.5 wt.% blend measured greater than 10^{13} ohms, and the resistance of resistors made from the 3 wt.% blend varied from 6×10^6 ohms to greater than 10^{13} ohms (the upper limit of our measurement capabilities). The blending curve of Figure 11 is not extended to the 2 vol.%; the sheet resistance of that composition is shown as extending from 6 megohms per square to 10^{17} ohms per square, the sheet resistance of the glass.

It must be realized that the blending curve shown in Figure 11 is not a unique curve for the RuO_2-glass system, rather, it applies only to the particular RuO_2 and glass powders used in this study. Powders with different average particle sizes and particle size distributions would give a different blending curve, particularly at the low RuO_2 end. The primary function of this experiment was to obtain a series of resistors having characterized electrical properties to be used in subsequent microstructure studies.

B. Effects of Substrate Expansion.

Since the inception of this program it has been planned to conduct a study to evaluate the effect of substrate-glass expansion mismatch on the resistance and TCR of thick film resistors []9]. A series of substrates with coefficients of linear thermal expansion in the range 2 to 10×10^{-6}/°C were obrained from American Lava. The substrates were flame sprayed with a thin coating of 96% alumina to assure that the resistor-substrate interface remained constant and hence, chemical effects

would not influence the results. The substrates shown in Table II were prepared.

Table II. Substrates for Thermal Expansion Experiment

ALSIMAG No.	Type	Nominal Composition	α_ℓ (ppm/°C)
447	Cordierite	$2MGO.2Al_2O_3.5SiO_2$	1.7
202	Cordierite	$2MgO.2Al_2O_3.5SiO_2$	2.8
475	Zircon	$ZrO_2.SiO_2$	4.9
614	Alumina	96% Al_2O_3	7.9
35	Steatite	$MgO.SiO_2$	8.5
243	Forsterite	$2MgO.SiO_2$	11.7

Platinum electrodes (Engelhard 6082) were printed on 6 different types of substrates and the firing was carried out at a peak temperature of 850°C. After this conductive firing it was discovered that the flame sprayed alumina coatings had broken away from substrates 447, 202 and 243, making further experiments with these three substrates impossible. Resistors were printed on substrates 475, 614, and 35; after firing it was discovered that all of the resistors on substrates 475 and 35 were cracked and the majority of the substrates of these two types showed marginal coating adherence. This left only the 614 substrate with measureable resistors, but this was the control. Hence, the experiment, as originally conceived, was a total failure. The thermal stresses developed at the interface between the flame sprayed coatings and the substrates were obviously too

large; it is still hoped that this experiment can be performed successfully, but the range of expansion coefficients must be narrowed so as to more closely match that of the 614 coating. In addition, the coating will be applied by the detonation gun process instead of flame spraying in order to obtain improved coating adhesion.

IV. Summary and Future Plans

A. Microstructure Development.

The sintering and ripening experiments described in this report will be continued until the various competing mechanisms are sorted out. The rate-limiting steps in the sintering and ripening processes will be established and the kinetic equations developed as a function of material properties. These are the remaining parameters needed to complete development of the phenomonological model for microstructure development.

B. Charge Transport.

Previously reported studies have shown that at least two types of charge transport processes are important in thick film resistors. Work will be completed on a statistical model of a thick film resistor which involves combinations of these mechanisms.

C. Final Report.

A final report will be prepared which will include a description of all experiments, a summary of experimental results, a description of the theoretical models, and a correlation of the models with the results.

V. REFERENCES

1. R. W. Vest, Semi-Annual Technical Report for the period 7/1/70-12/31/70, Purdue Research Foundation Grant No. DAHC-15-70-G7, ARPA Order No. 1642, Feb. 1, 1971.

2. R. W. Vest, Semi-Annual Technical Report for the period 7/1/71-6/30/71, Purdue Research Foundation Grant No. DAHC-15-70-G7, ARPA Order No. 1642, August 1, 1971.

3. R. W. Vest, Semi-Annual Technical Report for the period 7/1/71-12/31/71, Purdue Research Foundation Grant No. DAHC-15-70-G7, ARPA Order No. 1642, Feb. 1, 1972.

4. R. W. Vest, Semi-Annual Technical Report for the period 1/1/72-6/30/72, Purdue Research Foundation Grant No. DAHC-15-70-G7, ARPA Order No. 1642, August 1, 1972.

5. R. W. Vest, Semi-Annual Technical Report for the period 7/1/72-12/31/72, Purdue Rsearch Foundation Grant No. DAHC-15-70-G7, ARPA Order No. 1642, Feb. 1, 1973.

6. R. W. Vest, Semi-Annual Technical Report for the period 1/1/73-6/30/73, Purdue Research Foundation Grant No. DAHC-15-70-G7, ARPA Order No. 1642, August 1, 1973.

7. R. W. Vest, Semi-Annual Technical Report for the period 7/1/73-12/31/73, Purdue Research Foundation Grant No. DAHC-15-73-G8, ARPA Order No. 1001/192, Feb. 1, 1974.

8. R. W. Vest, Semi-Annual Technical Report for the period 1/1/74-6/30/74, Purdue Research Foundation Grant No. DAHC-15-73-G8, ARPA Order No. 1001/192, August 1, 1974.

References (cont'd)

9. Page 3, Reference 3.

10. Page 3-5, Reference 8.

11. Page 40-47, Reference 5; Page 33, Reference 1.

12. E. F. Kaeble, "Handbook of X-rays," McGraw-Hill, Inc., ppgs. 1-17, 1967.

13. R. I. Garrod, J. F. Brett and J. A. MacDonald, Australian J. Phys.

14. Page 17, Reference 8 7 (1), 77-95 (1954).

15. Page 19, Reference 8.

16. F. W. Jones, Proc. Roy. Soc. (London), 166A, 16 (1938).

17. Page 8, Reference 8.

18. Page 16-22, Reference 5.

19. Page 10-16, Reference 1.

20. Yasuro Nishimura, Kunihiko Asama and Hajime Sasaki, FUJITSU Scientific and Technical Journal, 159, March 1968.

21. Page 13-14, Reference 6.

22. Page 4, Reference 8.

23. Page 32, Reference 2.

24. Page 8-12, Reference 2.

25. Page 34-40, Reference 3.

26. Page 28-30, Reference 4.

27. Page 30-39, Reference 4.

28. Page 40, Reference 6.

29. Page 80, Reference 1.